

High-Resolution Measurements of Cyclic Adenosine Monophosphate Signals in 3D Microdomains

Jeffrey W. Karpen and Thomas C. Rich

Summary

A large number of hormones, neurotransmitters, and odorants exert their effects on cells by triggering changes in intracellular levels of cyclic adenosine monophosphate (cAMP). Although the effector proteins that bind cAMP have been identified, it is not known how this single messenger can differentially regulate the activities of hundreds of cellular proteins. It has been clear, for some time, that compartmentation of cAMP signals must be taking place, but the physical basis for compartmentation and the nature of local cAMP signals are mostly unknown. We present here a high-resolution method for measuring cAMP signals near the membrane in single cells. Cyclic nucleotide-gated (CNG) ion channels from olfactory receptor neurons have been genetically modified to improve their cAMP-sensing properties. We outline how these channels can be used in electrophysiological experiments to measure accurately changes in cAMP concentration near the membrane, where most adenylyl cyclases reside. We also describe how the method has been employed to dissect the roles of diffusion barriers and differential phosphodiesterase activity in creating distinct cAMP signals. This approach has much greater spatial and temporal resolution than other methods for measuring cAMP and should help to unravel the complexities of signaling by this ubiquitous messenger.

Key Words

Phosphodiesterase; adenylyl cyclase; cyclic nucleotide-gated ion channels; G protein-coupled receptors; second messengers; cyclic adenosine monophosphate (cAMP); subcellular compartmentation; diffusion; permeability barrier; biosensors.

1. Introduction

Cyclic adenosine monophosphate (cAMP), the prototypical second messenger, regulates a wide variety of cellular processes. Changes in cAMP concentration transmit information to downstream effectors including protein kinase A (PKA), cyclic nucleotide-gated (CNG) channels, hyperpolarization-activated

(I_hHCN) channels, and Epac (1–4). However, it is largely unclear how differential regulation of cellular targets occurs. The concept of compartmentation emerged more than 20 yr ago in studies of cardiac myocytes, to help explain how a variety of extracellular stimuli that primarily act through cAMP can have very different downstream effects on the cell (5,6). The basis for compartmentation and, indeed, the nature of cAMP signals themselves, have remained mysteries (7,8). To understand how these signals function within the cell, it is important to answer the following questions: (1) How are cAMP signals localized? (2) What are the kinetics of cAMP signals in localized domains? and (3) What information is contained in the amplitude and frequency of cAMP signals? To address these questions, olfactory CNG channels (CNGA2) have been adapted to measure cAMP in single cells (9–11) (see **Note 1**). There are several advantages to using genetically engineered CNG channels as high-resolution cAMP sensors: First, CNG channels are expressed in the plasma membrane, where most types of adenylyl cyclase (AC) are localized. Second, several hundred channels provide a readily detectable readout of cAMP concentration without significantly buffering the cAMP signal being measured (9,11,12). Third, CNG channels respond rapidly to changes in cyclic nucleotide concentration (9,12–14). Finally, the sensor can be calibrated in different cell types (9–11).

2. Materials

1. Adenovirus constructs for expression of CNG channels (pertinent characteristics of four CNG channel constructs used for monitoring cAMP levels are described in Chapter 4).
2. Primary or cultured cell lines in which measurements are to be conducted: The examples given here are in HEK-293 and C6-2B cells.
3. Minimal essential medium (MEM) supplemented with 26.2 mM NaHCO₃, 10% (v/v) fetal bovine serum (Gemini), penicillin (50 µg/mL), and streptomycin (50 µg/mL), pH 7.0, for HEK-293 cells, and F-10 medium supplemented with 26.2 mM NaHCO₃ and 10% bovine calf serum (Gemini), pH 7.0, for C6-2B cells.
4. 100 mM hydroxyurea stock solution: This is required only for cell lines in which adenovirus can readily replicate, including HEK-293 cells (see **Note 2**).
5. Electrophysiology setup for whole-cell and perforated patch-clamp experiments, and rapid perfusion system.
6. Extracellular buffer 1: 145 mM NaCl, 11 mM D-glucose, 10 mM HEPES, 4 mM KCl, and 0.1 mM MgCl₂, pH 7.4.
7. Extracellular buffer 2: 145 mM NaCl, 11 mM D-glucose, 10 mM HEPES, 4 mM KCl, and 10 mM MgCl₂, pH 7.4.
8. Perforated patch pipet buffer: 70 mM KCl, 70 mM potassium gluconate, 11 mM D-glucose, 10 mM HEPES, 4 mM NaCl, 0.5 mM MgCl₂, 1 mM cAMP, and 50–200 µg/mL of nystatin, pH 7.4 (see **Note 3**).

9. Whole-cell pipet buffer: 70 mM KCl, 70 mM potassium gluconate, 11 mM D-glucose, 10 mM HEPES, 4 mM NaCl, 0.5 mM MgCl₂, 5 mM K₂ATP, and 0.1 mM Na₂GTP, pH 7.4 (*see Note 4*).
10. Activators of adenylyl cyclase and inhibitors of phosphodiesterase (PDE). Add forskolin, prostaglandin E₁ (PGE₁), 3-isobutyl-1-methylxanthine (IBMX), and 4-(3-butoxy-4-methoxybenzyl)-2-imidazolidinone (RO-20-1724) to the control solution from concentrated dimethyl sulfoxide (DMSO) stocks, with the final concentrations as indicated (final DMSO concentrations were <0.5%).
11. Data analysis software: Appropriate software should be available from the manufacturer of the patch-clamp amplifier (e.g., Axon, Foster City, CA). We typically use the MATLAB software package (Mathworks, Natick, MA) to design custom analysis software in-house.

3. Methods

The following methods outline an approach to accurately measure cAMP concentrations near the surface membrane of living cells using modified olfactory CNG channels (*see Note 1*). This method offers unprecedented spatial and temporal resolution of cAMP signals. Among the findings with this approach are that cAMP in several cell types is produced in subcellular compartments under the plasma membrane with restricted diffusional access to the bulk cytosol, and that the amplitude and kinetics of cAMP signals within these compartments are distinct from those in the remainder of the cell (*see Note 5*).

3.1. Cell Culture and CNG Channel Expression

It is important to note that CNG channel expression in different cell types requires different multiplicity of infection (MOI) and incubation time. **Table 1** of Chapter 4 summarizes the conditions for optimal expression of CNG channels in several cell types.

1. Maintain HEK-293 and C6-2B cells in supplemented MEM and F-10 medium, respectively (*see Subheading 2., item 3*), in a humidified atmosphere of 95% air and 5% CO₂.
2. Plate the cells at approx 60% confluence in 100-mm culture dishes 24 h prior to infection with the CNG channel-encoding adenovirus constructs (MOI = 10 plaque-forming units/cell for HEK-293 cells and 100 for C6-2B cells).
3. When using adenovirus to transfect HEK-293 cells, add 2 mM hydroxyurea (final concentration) to the cell media 2 h postinfection to partially inhibit viral replication (*see Note 2*).
4. Twenty-four (HEK-293) or 48 h (C6-2B) postinfection, detach the cells with phosphate-buffered saline containing 0.03% EDTA (PBS-EDTA), resuspend in serum-containing medium, allow to recover for 1 h, and assay within 12 h. We use PBS-EDTA rather than trypsin-containing solutions so as not to modify extracellular regions of the CNG channels.

3.2. Measurement of Local cAMP in Single Cells

Single-cell cAMP measurements are made using either the perforated patch or whole-cell patch-clamp technique. A detailed consideration of patch-clamp methods is beyond the scope of this chapter, but there are excellent monographs and articles that provide a clear description of these electrophysiological approaches (15–17). Here, we focus on how patch-clamp techniques are used to measure the activity of CNG channel-based cAMP sensors, in order to measure cAMP concentrations near the surface membrane.

1. Pull patch pipets (electrodes) from borosilicate glass and heat polish. In our experiments, pipet resistance was limited to 5 M Ω and averaged 3.4 ± 0.5 M Ω (mean \pm SD).
2. Lower the pipets onto the cells and form gigaohm seals (8.3 ± 3.3 G Ω).
3. Make recordings using a patch-clamp amplifier (e.g., Axopatch-200A from Axon).
4. Digitize the signals corresponding to ionic currents and sample at five times the low-pass filter setting. For example, in some of our experiments, records were low-pass filtered with a 12-Hz bandwidth and sampled at 60 Hz.
5. Store and analyze the digitized records on a computer. In most cases records are later corrected for errors owing to series resistance (a combination of pipet resistance and access resistance to the cell interior).

3.2.1. Whole-Cell Experiments

In the whole-cell configuration, the piece of membrane underneath the patch pipet is ruptured by applying light suction or a brief electrical pulse (the “zap” feature available on most patch-clamp amplifiers). This allows dialysis of solutions from the patch pipet into the bulk cytosol. After achieving the whole-cell configuration, capacitive transients are elicited by applying 20-mV steps from the holding potential and recorded at 40 kHz (filtered at 10 kHz) for calculation of access resistance, which is typically <8 M Ω .

The whole-cell configuration is particularly useful for (1) washing in known concentrations of compounds that affect signal transduction (e.g., PDE inhibitors) into the cell, and (2) measuring the rate at which small molecules such as Na⁺ or cAMP wash into the cell and diffuse to their targets. The latter experiments can be used to estimate flux coefficients for the compartmental models described in **Subheading 3.4.**, or the effective diffusion coefficients of cAMP within the cell (9). For example, in HEK-293 cells, the wash in of Na⁺ from the patch pipet into the bulk cytosol is 90% complete in approx 22 s (9,18).

3.2.2. Perforated Patch Experiments

In the perforated patch configuration, the pore-forming antibiotic nystatin is added to the pipet solution to gain electrical access to the cell’s interior while retaining divalent cations and larger molecules such as cAMP in the cell (*see*

Note 3). A steady access resistance is obtained 5–15 min following seal formation. Capacitive transients are elicited by applying –30-mV steps from the holding potential of –20 mV for calculation of access resistance, typically less than 100 M Ω . These quantities are monitored throughout the experiments to ensure that stable electrical access is maintained. Solutions are applied using the SF-77B fast-step solution switcher (Warner, Hamden, CT) (*see Note 6*). In most of these experiments, 1 mM cAMP is included in the pipet solution; at the end of the experiment, the maximal cAMP-induced current can be measured by rupturing the cell membrane at the tip of the pipet with suction, allowing saturating cAMP to diffuse to the channels (**9**).

Examples of this technique are given in **Figs. 1** and **2**. In **Fig. 1** a single C6-2B cell expressing wild-type (WT) CNG channels (CNGB2; *see Note 1*) was stimulated with 50 μ M forskolin. This triggered a steady increase in inward current (measured at –50 mV). Currents were measured in 0.1 mM external MgCl₂ (extracellular buffer 1; *see Subheading 2., item 6*) and subsequently blocked by 10 mM external MgCl₂ (extracellular buffer 2; *see Subheading 2., item 7*) in a voltage-dependent fashion, a signature of currents through CNG channels. The ratio of the maximal forskolin-induced current to the maximal CNG channel current indicates that 50 μ M cAMP accumulated near CNG channels (*see Note 5*). In **Fig. 2A,B**, the responses of two different HEK-293 cells expressing C460W/E583M channels to rapid application of 1 μ M PGE₁ are shown. C460W/E583M channels can be used to measure cAMP signals at physiological concentrations (0.1–4 μ M) without significantly buffering the signal being measured; this is discussed in Chapter 4 and **refs. 11** and **12**. The inward currents through these channels were measured at a holding potential of –20 mV. Currents were converted to cAMP concentration based on the channel's dose-response relation as described in **Subheading 3.3**. Both the raw currents and the calibrated responses indicate that in response to PGE₁, cAMP levels increased transiently. We demonstrated that this transient response was owing to an initial increase in adenylyl cyclase activity followed by a more profound increase in PDE type IV activity (**11**). Interestingly, the total cellular cAMP levels rose to a steady plateau over the same time frame. To describe these results quantitatively, we used the framework of compartmental models discussed in **Subheading 3.4**.

3.3. Calibration of Single-Cell Measurements

The cyclic nucleotide sensitivity of WT and C460W/E583M CNG channels was assessed in excised, inside-out patches (**9,10**). The cAMP dose responses of these channels are fit with the Hill equation, $I/I_{\max} = [\text{cAMP}]^N / ([\text{cAMP}]^N + K_{1/2}^N)$, in which I/I_{\max} is the fraction of maximal current, $K_{1/2}$ is the cAMP concentration that gives a half-maximal current, and N is the Hill coefficient. We found

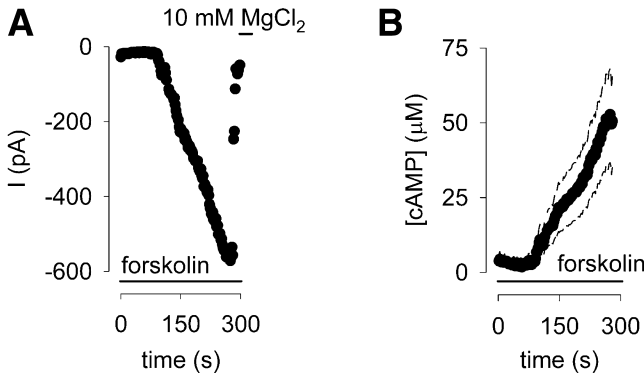


Fig. 1. cAMP measurements in a single C6-2B cell expressing WT CNG channels. (A) Response of a C6-2B cell to 50 μM forskolin (applied at time = 0), $V_m = -60$ mV, $I_{max} = 910$ pA. The response reached a plateau in approx 270 s. No forskolin-induced currents were observed in uninfected cells (cells not expressing CNG channels). (B) cAMP concentrations calculated using Hill equation (\bullet) \pm SD, based on uncertainty in calibration. (Reproduced from **ref. 9** by copyright permission of Rockefeller University Press.)

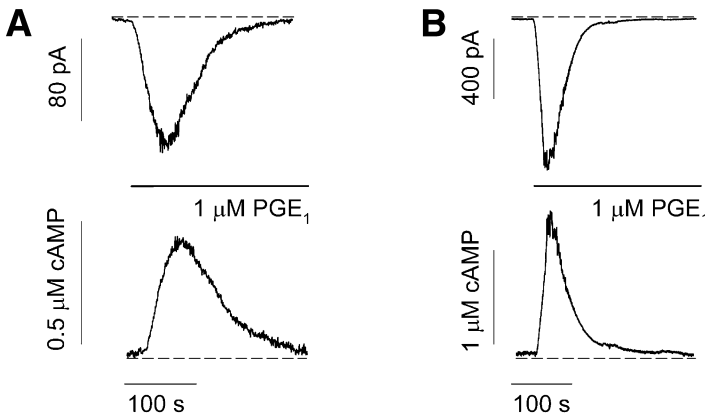


Fig. 2. Measurements of local cAMP signals in single HEK-293 cells. (A,B) At top, rapid application of PGE_1 triggered transient inward currents through C460/E583M CNG channels (-20 mV). (A) and (B) are the responses of two different cells. No PGE_1 -induced currents were observed in cells not expressing CNG channels. At bottom, the corresponding cAMP signals were calibrated as described in the text. Dashed lines indicate either zero cyclic nucleotide-induced current (the current in 10 mM $MgCl_2$) or zero cAMP. To maximize the response and remove the possibility of Ca^{2+} feedback, these experiments were conducted in nominally Ca^{2+} -free solutions (extracellular buffer 1; see **Subheading 2., item 6 [11]**).

the $K_{1/2}$ and N to be about 40 μM and 2.2 for the WT channels and 1.0 μM and 2.0 for the C460W/E583M channel (**10,11**). With these values, the cAMP concentration can be calculated from currents measured in perforated patch experiments (**9,11**). For example, if I/I_{\max} were found to be 0.6 in an experiment using C460W/E583M channels, the estimated cAMP concentration would be 1.2 μM . Note that the low concentration of channels expressed in these cells (~ 1 nM) does not significantly buffer the measured cAMP signals.

We confirmed this calibration technique in the whole-cell setting in two ways, measuring the responses induced by photolysis of caged cAMP and washing in different cAMP concentrations from the patch pipet into the cell (**9**).

3.4. Compartmental Models of Localized cAMP Signals

Several lines of evidence suggest that cAMP is produced in subcellular compartments near the surface membrane, and that diffusion between these domains and the bulk cytosol is significantly impeded (*see Note 5*) (**9,11**).

To describe these data quantitatively, we have used the framework of compartmental models. The major assumptions in these models are that each compartment is well mixed (the concentration within the compartment is uniform), and that there is a permeability barrier between compartments. This assumption is justified based on how rapidly cAMP diffuses without restriction across the entire cell (<0.2 s in a 20- μm -diameter cell).

We have used a simple compartmental model (**Fig. 3A**, inset) to describe several independent experimental observations. This model contains two compartments: a small subcellular compartment beneath the plasma membrane (compartment 1) whose volume is 2% of the bulk cytosol (compartment 2). In this model, PGE_1 triggers an increase in AC activity in compartment 1. PGE_1 also triggers an increase in PDE activity within compartment 1. This is consistent with our finding that the decline in the transient response (**Fig. 2**) is owing to a time-dependent upregulation of PDE type IV activity (**11**). The flux of cAMP from the microdomain to the bulk cytosol (from compartment 1 to compartment 2) is hindered by a permeability barrier. In addition, there is a constitutively active PDE in compartment 2.

The system is described by the following equations:

$$\frac{dC_1}{dt} = E_{AC} + \frac{J_{12}}{V_1} (C_2 - C_1) - \frac{A \cdot E_1 \cdot C_1}{K_{M1} + C_1} \quad (1)$$

$$\frac{dC_2}{dt} = \frac{J_{12}}{V_2} (C_1 - C_2) - \frac{E_2 \cdot C_2}{K_{M2} + C_2} \quad (2)$$

$$\frac{dA}{dt} = k_A I - k_I A \quad (3)$$

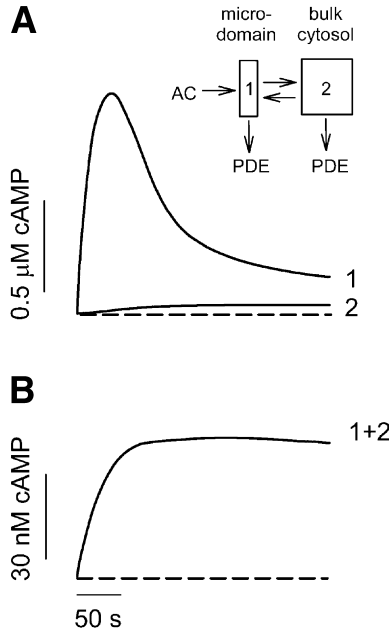


Fig. 3. Quantitative description of localized transient cAMP response and total cellular cAMP accumulation. The inset shows a two-compartment model of the cell with a diffusional restriction between the membrane-localized microdomain (compartment 1) and the bulk cytosol (compartment 2). See the text for details. (A) Rapid activation of AC and slower activation of PDE shape the transient signal in the microdomain. The slow flux of cAMP from the microdomain allows low levels to accumulate in the cytosol. Even in the small volume of the microdomain, the concentration of CNG channels is low (~ 40 nM) and will not significantly buffer the cAMP signal. (B) Total cAMP levels (microdomain and cytosol) reach a plateau. Dashed lines indicate zero cAMP (II).

in which V_1 and V_2 are the volumes of compartments 1 and 2, respectively; C_1 and C_2 are the cAMP concentrations; J_{12} is the flux coefficient between compartments; E_{AC} is the synthesis rate of cAMP; E_1 and E_2 are the maximal cAMP hydrolysis rates; K_{M1} and K_{M2} are the Michaelis constants for PDE activity; A and I are the fraction of active and inactive PDE in compartment 1, respectively ($A + I = 1$); and k_A and k_I are the rate constants of PDE activation and inactivation, respectively. $J_{12} = 8.0 \times 10^{-16}$ L/s, $V_1 = 0.040$ pL, and $V_2 = 2.0$ pL. AC activity is considered constant, with $E_{AC} = 0.13$ $\mu\text{M/s}$. K_{M1} , E_1 , K_{M2} , and E_2 are 0.30 μM , 0.83 $\mu\text{M/s}$, 1.0 μM , and 0.0020 $\mu\text{M/s}$, respectively. The rate constants k_A and k_I are 0.0015 s^{-1} and 0.0010 s^{-1} , respectively. The initial and final (300 s) values of A are 0.10 and 0.36, respectively. The parameters used in this simulation reflect similar total PDE activities near the plasma membrane and

throughout the cytosol. This is in broad agreement with the findings of experiments on PDE type IV in several cell types (**19**).

Simulations of the model successfully reproduce the local transient change in cAMP, as well as the rise in total cAMP to a plateau (**Fig. 3**). A PGE₁-induced increase in PDE activity within compartment 1 is required to explain the data. Slow efflux of cAMP from the microdomain is ultimately balanced by low rates of hydrolysis within the bulk cytosol. Thus, different relative PDE activities within more than one diffusionally restricted compartment can explain the generation of distinct cAMP signals (*see* **Note 7**).

4. Notes

1. This approach was inspired by the field of retinal phototransduction, the best-studied second-messenger signaling system, in which elegant biochemical studies have been complemented by real-time measurements of cyclic guanosine 5'-monophosphate (cGMP) signals using endogenous CNG channels (**20–23**). CNG channels are directly opened by the binding of cyclic nucleotides. They were discovered in retinal photoreceptor cells and olfactory receptor neurons, where they generate the electrical response to light and odorants. The native retinal channel is cGMP specific, whereas the native olfactory channel is equally sensitive to cAMP and cGMP. Native CNG channels consist of A- and B-subunits, both of which bind cyclic nucleotides, although most A-subunits form functional channels on their own. We have modified an olfactory channel A-subunit (CNGA2) to improve its sensitivity and selectivity for cAMP.
2. Higher hydroxyurea concentrations (≥ 10 mM) are required to completely inhibit viral replication. However, such high concentrations affect cellular adenosine triphosphate (ATP) pools and can significantly alter second-messenger signaling. We have determined that 1 to 2 mM hydroxyurea sufficiently inhibits viral replication without significantly altering ATP pools in HEK-293 cells. As a further control for potential effects of hydroxyurea, the experiments described here can be repeated with CNG channels expressed using other transfection techniques such as Ca₃(PO₄)₂ precipitation (**24**). We have done these controls and found that the lower hydroxyurea concentrations have little or no effect on cAMP signals (**9–11**). It is important to note that we use adenovirus to transfect cells because it allows relatively uniform CNG channel expression in a majority ($\geq 70\%$) of cells.
3. In the perforated patch configuration, pipet solutions contained nystatin (diluted from 50 mg/mL stock in DMSO) to gain electrical access to the cell. These solutions were kept on ice and shielded from light until use. Using this approach, the solutions can be used for 4–8 h. We fill the entire pipet with nystatin-containing solution (*see* **Subheading 2., item 8**). In our hands this does not impede seal formation. In general, we start each day using low nystatin concentrations (50 μ g/mL). A steady access resistance is typically obtained 5–15 min following seal formation. If low access resistances (< 100 M Ω) are not readily achieved with this solution, we use a higher nystatin concentration (100 μ g/mL). Nystatin did

not induce measurable currents up to 20 min after break-in in whole-cell experiments; this is of particular importance for the single-cell calibration of cAMP concentrations.

4. If one is studying only forskolin activation of adenylyl cyclase in the whole-cell configuration, it may be beneficial to omit Na_2GTP from the patch pipet solution. This will minimize/eliminate G protein-mediated signaling from the preparation.
5. Several lines of evidence using CNG channels as biosensors in HEK-293 and C6-2B glioma cells point to the existence of a barrier under the surface membrane that significantly hinders the diffusion of cAMP into the rest of the cell: First, stimulation of membrane adenylyl cyclase with forskolin causes cAMP to build to much higher concentrations near the surface membrane than throughout the cell (>12-fold difference). The proximity of the sensor to adenylyl cyclase cannot explain this observation. In effect, in the absence of a diffusion barrier, each cAMP would diffuse away faster than the next one is produced (9). Second, rapid dialysis of the bulk cytosol in the whole-cell patch configuration (as opposed to the perforated patch configuration) does not measurably alter the magnitude or kinetics of cAMP accumulation near the membrane (9). Third, the wash in of cAMP from the patch pipet to the CNG channels (in the whole-cell configuration) is considerably slower than would be expected compared to the wash in of other small molecules (9,18). These observations led to the prediction that distinct cAMP signals could coexist within a cell. Such distinct signals have been resolved in PGE_1 -stimulated HEK-293 cells (see Figs. 2 and 3) (11). So far the evidence for a diffusional restriction is solely from functional measurements. The biochemical and morphological basis for the barrier(s) remains to be determined. This is a fascinating subject for future study.
6. The mechanical switch time was 1 ms for the SF-77B fast-step solution switcher (Warner). The time to exchange the extracellular solution was measured by applying a 140 mM KCl solution to a depolarized HEK-293 cell (+50 mV), and monitoring changes in current through endogenous voltage-gated K^+ channels; for each experiment, it was <60 ms.
7. Recently, the subcellular localization of cAMP signals has become a topic of much discussion (5,7,8). The frequency of cAMP signals is also likely to be important in the regulation of downstream targets (12,25,26). The downstream targets of cAMP signals have vastly different apparent cAMP affinities and activation/deactivation kinetics. For example, PKA has a high apparent affinity for cAMP and relatively slow reassociation rates. This indicates that PKA will remain active after cAMP levels decline (12). By contrast, CNG channels have a relatively low apparent cAMP affinity and fast kinetics. Thus, CNG channel activity will follow the time course of cAMP signals at frequencies as high as 10 Hz. It is unlikely that the different properties of these enzymes are accidental. Rather, they may have evolved to respond to different amplitudes and frequencies of cAMP signals. Indeed, it is likely that differential regulation of distinct types of PDE by a variety of intracellular messengers will be required in order to encode

information in a frequency-dependent manner. Chapters 5, 10–14, and 16–21, in this volume outline a variety of approaches to examine the regulation of PDE activity in vitro; however, these approaches cannot determine whether frequency encoding of information occurs in living cells. Thus, high-resolution, single-cell measurements of cAMP signals are required to test this hypothesis.

References

1. Montminy, M. (1997) Transcriptional regulation by cyclic AMP. *Annu. Rev. Biochem.* **66**, 807–822.
2. Francis, S. and Corbin, J. D. (1999) Cyclic nucleotide-dependent protein kinases: intracellular receptors for cAMP and cGMP action. *Crit. Rev. Clin. Lab. Sci.* **36**, 275–328.
3. Finn, J. T., Grunwald, M. E., and Yau, K.-W. (1996) Cyclic nucleotide-gated ion channels: an extended family with diverse functions. *Annu. Rev. Physiol.* **58**, 395–426.
4. de Rooij, J., Zwartkruis, F. J., Verheijen, M. H., Cool, R. H., Nijman, S. M., Wittinghofer, A., and Bos, J. L. (1998) Epac is a Rap1 guanine-nucleotide-exchange factor directly activated by cyclic AMP. *Nature* **396**, 474–477.
5. Steinberg, S. F. and Brunton, L. L. (2001) Compartmentation of G protein-coupled signaling pathways in cardiac myocytes. *Annu. Rev. Pharmacol. Toxicol.* **41**, 751–773.
6. Jurevicius, J. and Fischmeister, R. (1996) cAMP compartmentation is responsible for a local activation of cardiac Ca^{2+} channels by β -adrenergic agonists. *Proc. Natl. Acad. Sci. USA* **93**, 295–299.
7. Karpen, J. W. and Rich, T. C. (2001) The fourth dimension in cellular signaling. *Science* **293**, 2204, 2205.
8. Hall, D. D. and Hell, J. W. (2001) The fourth dimension in cellular signaling—response. *Science* **293**, 2205.
9. Rich, T. C., Fagan, K. A., Nakata, H., Schaack, J., Cooper, D. M. F., and Karpen, J. W. (2000) Cyclic nucleotide-gated channels colocalize with adenylyl cyclase in regions of restricted cAMP diffusion. *J. Gen. Physiol.* **116**, 147–161.
10. Rich, T. C., Tse, T. E., Rohan, J. G., Schaack, J., and Karpen, J. W. (2001) In vivo assessment of local phosphodiesterase activity using tailored cyclic nucleotide-gated channels as cAMP sensors. *J. Gen. Physiol.* **118**, 63–77.
11. Rich, T. C., Fagan, K. A., Tse, T. E., Schaack, J., Cooper, D. M. F., and Karpen, J. W. (2001) A uniform extracellular stimulus triggers distinct cAMP signals in different compartments of a simple cell. *Proc. Natl. Acad. Sci. USA* **98**, 13,049–13,054.
12. Rich, T. C. and Karpen, J. W. (2002) Cyclic AMP sensors in living cells: what signals can they actually measure? *Ann. Biomed. Eng.* **30**, 1088–1099.
13. Karpen, J. W., Zimmerman, A. L., Stryer, L., and Baylor, D. A. (1988) Gating kinetics of the cyclic-GMP-activated channel of retinal rods: flash photolysis and voltage-jump studies. *Proc. Natl. Acad. Sci. USA* **85**, 1287–1291.
14. Hagen, V., Dzeja, C., Frings, S., Bendig, J., Krause, E., and Kaupp, U. B. (1996) Caged compounds of hydrolysis-resistant analogues of cAMP and cGMP: synthesis and application to cyclic nucleotide-gated channels. *Biochemistry* **35**, 7762–7771.

15. Sakmann, B. and Neher, E. (1995) *Single Channel Recording*, Plenum, New York.
16. Hille, B. (2001) *Ionic Channels of Excitable Membranes*, Sinauer, Sunderland, MA.
17. Horn, R. and Marty, A. (1988) Muscarinic activation of ionic currents measured by a new whole-cell recording method. *J. Gen. Physiol.* **92**, 145–159.
18. Pusch, M. and Neher, E. (1988) Rates of diffusional exchange between small cells and a measuring patch pipette. *Pflügers Arch.* **411**, 204–211.
19. Houslay, M. D., Sullivan, M., and Bolger, G. B. (1998) The multienzyme PDE4 cyclic adenosine monophosphate-specific phosphodiesterase family: intracellular targeting, regulation, and selective inhibition by compounds exerting anti-inflammatory and antidepressant actions. *Adv. Pharmacol.* **44**, 225–342.
20. Stryer, L. (1991) Visual excitation and recovery. *J. Biol. Chem.* **266**, 10,711–10,714.
21. Yau, K.-W. (1994) Phototransduction mechanism in retinal rods and cones: The Friedenwald Lecture. *Invest. Ophthalmol. Vis. Sci.* **35**, 9–32.
22. Molday, R. S. (1998) Photoreceptor membrane proteins, phototransduction, and retinal degenerative diseases: The Friedenwald Lecture. *Invest. Ophthalmol. Vis. Sci.* **39**, 2493–2513.
23. Kaupp, U. B. and Seifert, R. (2002) Cyclic nucleotide-gated ion channels. *Physiol. Rev.* **82**, 769–824.
24. Jordan, M., Schallhorn, A., and Wurm, F. M. (1996) Transfecting mammalian cells: optimization of critical parameters affecting calcium-phosphate precipitate formation. *Nucleic Acids Res.* **24**, 596–601.
25. Rapp, P. E. and Berridge, M. J. (1977) Oscillations in calcium-cyclic AMP control loops form the basis of pacemaker activity and other high frequency biological rhythms. *J. Theor. Biol.* **66**, 497–525.
26. Cooper, D. M. F., Mons, N., and Karpen, J. W. (1995) Adenylyl cyclases and the interaction between calcium and cAMP signalling. *Nature* **374**, 421–424.



<http://www.springer.com/978-1-58829-314-5>

Phosphodiesterase Methods and Protocols

Lugnier, C. (Ed.)

2005, 336 p. 93 illus., 1 illus. in color., Hardcover

ISBN: 978-1-58829-314-5

A product of Humana Press